THE JOURNAL OF PHYSICAL CHEMISTRY B

Article

pubs.acs.org/JPCB

Membrane Permeation of a Peptide: It Is Better to be Positive

Alfredo E. Cardenas,*[,†] Rebika Shrestha,[‡] Lauren J. Webb,[‡] and Ron Elber[†,‡]

[†]Institute for Computational Engineering and Sciences and [‡]Department of Chemistry, University of Texas at Austin, Austin, Texas 78712, United States

ABSTRACT: A joint experimental and computational study investigates the translocation of a tryptophan molecule through a phospholipid membrane. Time dependent spectroscopy of the tryptophan side chain determines the rate of permeation into 150 nm phospholipid vesicles. Atomically detailed simulations are conducted to calculate the free energy profiles and the permeation coefficient. Different charging conditions of the peptide (positive, negative, or zwitterion) are considered. Both experiment and simulation reproduce the qualitative trend and suggest that the fastest permeation is when the tryptophan is positively charged. The permeation mechanism, which is revealed by molecular dynamics simulations, is of a translocation assisted by a local defect. The influence of long-range electrostatic interactions, such as the membrane dipole potential on the permeation process, is not significant.

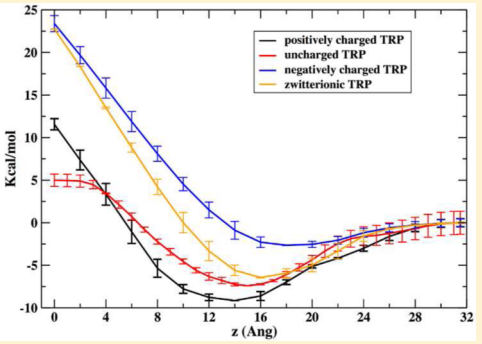

I. INTRODUCTION

The cell membrane is the natural barrier that separates the interior of the cell from the extracellular environment. This barrier is essential for life, retaining necessary concentration gradients and separating ingredients for biochemical reactions from waste products and undesired chemicals. One of the most important concentration gradients is of ions, maintaining an electric field across biological membranes. This field is vital, and living systems invest significant biological machinery (pumps) and energy to maintain it.[1] It is therefore of considerable interest to quantify the rate of ion "leakage" through membranes, i.e., the rate in which ions permeate through biological membranes without assistance. The unassisted permeation follows the opposite direction of the concentration gradient. It is against this leakage that the cell must continuously struggle and pump back ions, a struggle that will stop only at cell death.

Molecular dynamics simulations have been used to provide an atomically detailed view of the insertion and translocation of charged species through model lipid bilayers. The first estimates of the potential of mean force (PMF) along the membrane axis (the normal to the membrane surface) for monatomic ions using atomically detailed simulations go back to Wilson and Pohorille, who obtained an energy barrier located at the membrane center of about 54 kcal/mol for Na^+ and 50.5 kcal/mol for Cl^- ions.[2] Later, Tepper and Voth[2] using a multistate variant of the empirical valence bond model[3] estimated barriers for ion leakage for H^+, OH^-, and Na^+ (for the latter, the barrier was 24 kcal/mol). More recently, McCammon et al.[4] in a study of ion-pairing reported barriers for permeation of 21.9 kcal/mol for Na^+, 23.6 kcal/mol for Cl^-, and 27.6 kcal/mol for the Na^+–Cl^- ion pair.

Molecular dynamics simulations have also been used to study mechanisms and energetics of permeation of more complex biological molecules such as charged amino acids. Amino acid and peptide translocation are useful in modeling the mechanism of peptide and of protein insertion to membranes.[5] Arginine was studied most extensively due to its significant role in cell permeating peptides (CPPs).[6,7] Several simulations have shown that arginine remains positively charged even at the center of the bilayer.[8−10] Other charged side chains have higher barriers. Tieleman computed a barrier of about 14 kcal/mol for the side chain of arginine, 20 kcal/mol for the side chain of glutamic acid, and 19 kcal/mol for the side chain of aspartic acid.[8] Allen et al.[11] computed the PMF of analogues of lysine and arginine and estimated that charged arginine can permeate through the membrane but not charged lysine. Recent experiments have confirmed those findings.[12]

All of these atomically detailed simulations of atomic ions or charged amino acid analogues show that the permeation of these species affects the membrane structure. When the ion moves inside the membrane, it remains partially or fully hydrated and is not impacted in a significant way by the dipole potential of the membrane that in its unperturbed form favors permeation of anions over cations.[13,14]

When considering permeation through membranes of complex molecules, it is difficult to separate the impact of charge from variations in molecular size and flexibility. The permeation mechanism that prefers positively charged amino acids versus negatively charged residues is therefore not clear. To address this question, we consider the translocation of the same amino acid under different pH conditions. The particular study of tryptophan was motivated by its abundance in membrane proteins as an interfacial anchor and ease of detection by spectroscopic means. We used experiments and simulations to measure the permeation amplitude and rate of a

Received: March 4, 2015
Revised: April 30, 2015

DOI: 10.1021/acs.jpcb.5b02122
J. Phys. Chem. B XXXX, XXX, XXX−XXX

single amino acid tryptophan through DOPC membrane. In the simulations, we assumed that the prime effect of pH changes is to modify the charges of the zwitterionic amino acid. Both simulations and experiments indicate that it is the positively charged ion of the tryptophan species that permeates through the membrane most efficiently.

II. METHODS

II.1. Experiments. *II.1.1. Materials and Methods.* 1,2-Dioleoyl-*sn*-glycerol-3-phosphocholine (DOPC, dissolved in chloroform) was purchased from Avanti Polar Lipids, Inc. L-Tryptophan, HEPES buffer, and NaN_3 were purchased from Sigma-Aldrich; citric acid monohydrate, sodium bicarbonate ($NaHCO_3$), and sodium carbonate anhydrous ($NaCO_3$) were purchased from Fisher Scientific; and anhydrous sodium phosphate (Na_2HPO_4) was purchased from Mallindkrodt Pharmaceuticals. Buffers of various pH values were prepared in HPLC grade water purchased from Fischer Scientific. All chemicals were used as received unless noted.

II.1.2. Vesicle Preparation. Large unilamellar vesicles were prepared using an extrusion method. A 945 μL portion of DOPC lipid in chloroform (25 mg/mL) was dried under a vacuum for at least 2 h and placed in a N_2(g)-purged glovebox overnight to get rid of any residual solvent. The dried lipids were hydrated in 1.0 mL of 10 mM Hepes buffer with 0.02% NaN_3, pH 7.2, for at least 30 min and agitated vigorously using a vortex mixer for 5 min. The hydrated lipid suspension was then subjected to at least 10 cycles of a freeze−thaw process consisting of alternately placing the sample vial in liquid N_2 and a warm water bath. The lipid suspension was then loaded into a gas-tight syringe of a mini-extruder (Avanti Polar Lipids) and extruded through a membrane of 100 nm pore size 20 times, during which time the milky solution visibly cleared. The large unilamellar vesicles were then collected in a vial and stored at room temperature for further usage. For pH experiments, vesicles were prepared in three other buffers at pH 10.1 (0.1 M Na_2CO_3, 0.1 M $NaHCO_3$), pH 5.5 (0.1 M citric acid, 0.2 M Na_2HPO_4), and pH 2.4 (0.1 M citric acid, 0.2 M Na_2HPO_4). Control experiments in which the concentration of the buffer was halved while retaining the same pH were conducted as well. The average diameter of vesicles was determined to be 150 ± 17 nm using a Malvern Zetasizer Nano ZS instrument equipped with a He−Ne laser light source to illuminate the sample at a wavelength of 633 nm and collected at a scattering angle of 173°. All measurements were made at a temperature of 35 °C, viscosity of 0.8872 cP, refractive index of 1.330, equilibration time of 120 s, and path length of 1 cm.

II.1.3. Amino Acid Permeation through a Bilayer. A 100 μL portion of vesicle suspension was mixed with 300 μL of 10 mM tryptophan in the appropriate buffer (described previously) maintained at 27 °C for up to 24 h. At a series of time points ranging from 5 to 60 min and 2 to 24 h, the solution was passed through a PD-10 desalting column (GE Healthcare) containing 8.3 mL of Sephadex G-25 medium previously equilibrated with the same buffer. Small molecules such as free tryptophan that had not diffused into the bilayer were trapped within the pores of the column, while the large vesicles were eluted out and collected in a vial. Fluorescence measurements of tryptophan associated with these vesicles were made with a Synergy H4 Fluorimeter set to an excitation wavelength of 280 nm and emission wavelength of 348 nm.

II.1.4. Rate Constant and Permeability Coefficient Calculation. The kinetics of tryptophan permeation into the vesicle bilayer was determined by fitting the change in fluorescence over length of time to eq 1[15,16]

$$[F(t)]_i = [F(\mathrm{eq})]_i(1 - \mathrm{e}^{-kt}) \quad (1)$$

where $[F(t)]_i$ is the fluorescence from amino acids inside the vesicles at time t, $[F(\mathrm{eq})]_i$ is the fluorescence from amino acids at equilibrium inside vesicles at $t = \infty$, and k is the permeation rate constant. The permeability coefficient (P) under different pH conditions requires more elaborate analysis and assumptions motivated by (current) experimental and computational observables. We therefore will discuss the calculation of P in the Results and Discussion section.

II.2. Simulations. In all simulations, the periodic box contains a total of 40 DOPC molecules (20 in each leaflet), 1542 water molecules, and 1 or 2 tryptophan molecules. For the charged tryptophan species (positively or negatively charged amino group or the zwitterionic molecule), only one permeant was added in the simulation box. For the uncharged neutral species, two tryptophan molecules were added in the box, one in each leaflet making sure that the separation of their center of masses was always greater than 32 Å. When needed, an additional counterion (chloride or sodium ions) was added to the aqueous solution to keep the electroneutrality of the simulation box.

The simulations were performed at a constant temperature of 300 K and constant volume. The cell size is 37 × 37 × 75 Å^3 with the z axis (perpendicular to the membrane surface) corresponding to the largest side. The area per lipid is 68.5 Å^2, close to the reported experimental value of 72.1 Å^2 for DOPC membrane bilayers.[17] All of the permeants were modeled with the OPLS united-atom force field,[18] and a combination of Berger/OPLS parameters was used for the lipid molecules.[19] The SPC model was used to represent the water molecules.[20] We applied periodic boundary in the three spatial directions. The long-range electrostatics interactions were computed with the smooth particle mesh Ewald method[21] with 32 × 32 × 64 cubic grids. The cutoff for the real component of the electrostatic potential and the van der Waals interactions was set to 9.0 Å. We used a matrix implementation of SHAKE to constrain water bond lengths and angles.[22,23] We employed r-RESPA[24] to integrate the equations of motion with a short time step of 1 fs to evaluate the covalent, van der Waals, and real component of the electrostatics interactions, and a longer time step of 4 fs to estimate the reciprocal space component of the Ewald sum.[52]

The initial configurations were taken from previously performed simulations of a terminally blocked tryptophan (NATA) permeation through a bilayer membrane of DOPC molecules.[25] In the current simulation, the NATA molecule was replaced for any of the four different tryptophan species considered here. After an initial 500 ps equilibration period, production jobs of 50 ns were launched in each of the umbrella windows considered. We used a harmonic potential to constrain the position of the center of mass of the permeants on 33 windows along the membrane axis (z axis). The separation between consecutive windows was 2 Å, and the harmonic force constant applied was of 7 kcal/mol. For windows closer to the membrane center (4 Å away from the center), the simulations of the charged tryptophan species were extended to 90 ns to improve the convergence of the structural results at those membrane depths. Convergence was assessed by comparison of the results of independent simulations for the two membrane layers. We use the z-constraint method[26,27] to

DOI: 10.1021/acs.jpcb.5b02122
J. Phys. Chem. B XXXX, XXX, XXX−XXX

obtain the potential of mean force and permeability estimates for membrane permeation of the different tryptophan moieties.

We further evaluate the sampling using ergodic measures we have employed in the past.[28,29] In Figure 1, we illustrate that the mean force appeared to be sampled from a normal distribution after about 30 ns, suggesting uniform sampling and lack of drift.

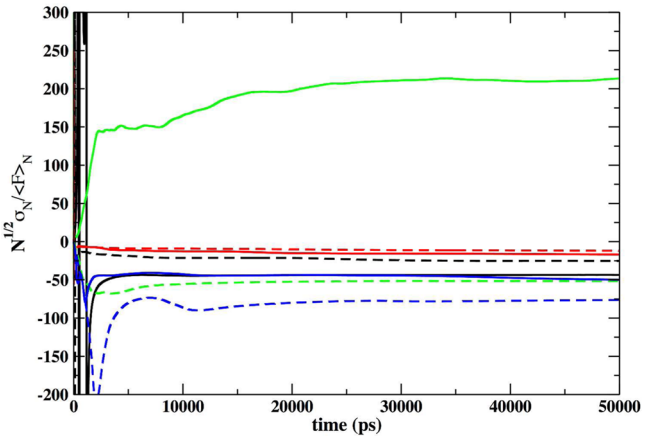

Figure 1. Product of the square root of the number of data points N times the ratio of the variance of the constrained force σ to the average $\langle F\rangle_N$ along the membrane axis. Results are shown for four windows along the membrane axis: window at z = 0 Å (black), 8 Å (red), 16 Å (green), and 24 Å (blue). Solid lines are for positively charged tryptophan and dashed lines for negatively charged tryptophan.

III. RESULTS AND DISCUSSION

The prime goal of the present manuscript is to examine mechanisms of passive transport of charged and moderately complex molecules through the membrane. The questions that we address are the following: (i) Is the permeation through the hydrophobic core of the membrane bilayer possible at all reasonable conditions? We illustrate below that such permeation is measurable experimentally at the minute to hour time scale and is feasible according to computer simulations. Therefore, we continue to ask: (ii) Given that the overall shape of the permeant is fixed and only the charge is changing, what is the impact of charge variation on the permeability? Finally, (iii) what is the molecular mechanism of the passive permeation of these charged molecules?

III.1. Experimental Evidence for Translocation through a Membrane of Permeants with Different Charges and Highly Similar Molecular Structures. In Figure 2, we show measurements of tryptophan permeation as a function of time for different pH conditions. It is assumed that the changes of the pH do not significantly affect the permeation properties of the membrane. Recall that the experiments first place the phospholipid vesicles in tryptophan solution, allowing the solute to permeate the membrane for a fixed period of time. The solution is then washed away, and the amount of permeating tryptophan is assessed and reported in units of nanomoles (nmol). While the measurement time scale is rather slow on the molecular time scale (minutes and hours) and it is difficult to resolve the initial rise of tryptophan concentration in the DOPC vesicles, the differences in the long time amplitudes are obvious. It is clear that at low values of pH we obtain a significantly larger amount of positively charged tryptophan

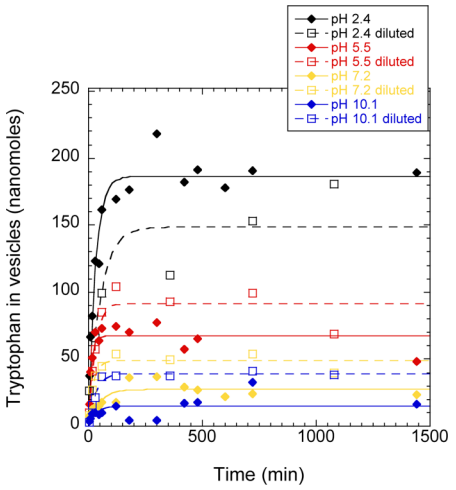

Figure 2. Permeation of tryptophan through a DOPC membrane under different pH conditions. It is evident that the amount of tryptophan released is the highest at low pH levels, suggesting that permeation at low pH and positive charge is fastest. The unfilled squares are the results of experiments conducted with diluted buffer. See text for more details. The solid and dashed lines are exponential fittings to the experimental data points for undiluted and diluted buffers, respectively.

molecules (black diamonds) permeating to the vesicle than for the zwitterionic (yellow diamonds) or negatively charged peptide (blue diamonds).

This result is surprising if we use the simplest model of a membrane as a thin hydrophobic layer in aqueous solution. Such a layer is not expected to select a particular charge that we illustrate in this manuscript for the DOPC membrane. As surprising as this result might be, there is already considerable experimental evidence and theoretical studies illustrating selectivity of charges by membrane. Clarke[13] argued that a dipole electric field across the membrane assists the permeation of a particular type of charged systems, namely, organic ions.[30] He made a reference to interesting experiments comparing the permeation of aromatic charges tetraphenylborate and tetraphenylphosphonium.[31] The experiment by Liberman and Topaly suggests that the partition coefficients of the anions in the membrane are 10^5 times larger than the partition coefficients of the cations. These two ions have comparable sizes but opposite charges, and hence the suggestion that the prime force controlling the difference in their permeation rates must be electrostatic. Clarke proposed a mechanism for this surprising phenomenon and attributed the differences to favorable interactions of the membrane dipole moment with anions.[13]

There are several questions that the Clarke model raises that we address in this manuscript: (i) Is the electric field of pure membrane indeed following the Clarke prediction (i.e., more favorable for negative ions), and if yes, why and what is its origin? (ii) Is the model that successfully explained the permeation of organic ions applicable to more typical biological molecules such as peptides? (iii) Are there alternative molecular mechanisms favoring different charge permeation?

One of the more popular amino acids found in peptides (such as CPP) designed to permeate membranes is arginine, which is positively charged at variance with Clarke arguments. Permeations of arginine amino acids or side chains were illustrated computationally and experimentally.[8,11,12,32−34] On

DOI: 10.1021/acs.jpcb.5b02122
J. Phys. Chem. B XXXX, XXX, XXX−XXX

the other hand, arginine experiments are not necessarily a measure of the charge effect on permeation. For example, it is possible that the long hydrophobic chain of arginine facilitates its permeation and not necessarily the charge, which is the focus of our discussion here. What we miss in this case is a comparative study to an anion with similar structural features to arginine.

To address the impact of charges and permeation of peptides, studies that are relevant also to the insertion of trans-membrane proteins, we consider the permeation of tryptophan under different pH conditions. Variation of pH does not significantly affect the shape of this single amino acid. However, it impacts the charge. At low pH values, the N terminal is mostly positively charged while the C terminal is neutral. At moderate pH, tryptophan is zwitterionic, and at high pH, the C terminal is mostly negatively charged.

Indeed, the experimental permeation curves in Figure 2 show a profound impact of the pH on the permeation rates. The number of permeating molecules (the amplitude of the kinetic curve) is significantly affected by the charge state. Figure 2 clearly illustrates more efficient permeation to the vesicle by a tryptophan solution enriched with positively charged peptides. This is in contrast with the prediction of the theory of the membrane electric dipole by Clarke[13] and in agreement with simulations and experiments on arginine residues[8,11,32] and CPP.[6,35] Nevertheless, the data is noisy and the rapid rise at early times on the experimental time scale makes it difficult to determine if the kinetics is exponential and if it is exponential what is the rate coefficient.

To test the sensitivity of the results to buffer conditions, we repeat the experiments by halving the concentrations of the buffer while keeping the system at the same pH (Figure 2). The ionic strength influences permeation in a complex way. When the ionic strength decreases, it makes permeation slower for pH 2.4 and faster at pH 5.5. Our analysis focuses on the undiluted data for which the results are less noisy. The main conclusion of the paper that the positively charged species is permeating faster remains unaffected.

Despite these difficulties, we have attempted to quantitatively model the experimental data. We make the following assumptions to simplify the analysis and reduce the number of parameters required: (i) The changes in the pH influence only the peptide charge and not other features of the system (e.g., the overall structure of the membrane is not affected). (ii) The permeant species is primarily the positively charged tryptophan. The last assumption is motivated by the experimental observation showing significantly large permeability at low pH but little variation in the rate coefficient at different pH as estimated by an exponential fit of the experimental curves. The second assumption is also supported by the simulation results that predict that only the positive species is permeating (see next section). The equations below of mass balance and pH impact on permeation are similar to the discussion by Cullis et al.;[36] however, they did not consider the permeation dependence on the type of the charge.

At any pH, the total concentration of the tryptophan molecules is a combination of three species: $[TRP] = [P^+] + [N^-] + [Z^{+/-}]$, where $[P^+]$ is the protonated, low pH, positively charged species, $[N^-]$ is the high pH, negatively charged species, and $[Z^{+/-}]$ is the zwitterion form. The equilibrium relationships in aqueous solution between the three species are given by

$$P^+ \rightleftarrows Z^{+/-} + H^+ \quad K_1 = \frac{[Z^{+/-}][H^+]}{[P^+]} \quad K_1 = 4.17 \times 10^{-3}$$

$$Z^{+/-} \rightleftarrows N^- + H^+ \quad K_2 = \frac{[N^-][H^+]}{[Z^{+/-}]} \quad K_2 = 4.07 \times 10^{-10} \tag{2}$$

Using the second assumption that the dominating permeating species is the positively charged ion $[P^+]$, we can write for the kinetics of the change of the tryptophan concentration outside of the vesicle

$$\frac{d[TRP]}{dt} = \frac{d[P^+]}{dt} \tag{3}$$

Let the volume of the experimental apparatus be V. The total number of tryptophan molecules is $N = [TRP]\cdot V$. One definition of the permeability coefficient (P) is

$$\frac{d[TRP]\cdot V}{dt} = -PA([P^+] - [P^+_{inside}]) \tag{4}$$

where A is the total accumulated surface areas of all the vesicles in solution. Initially, the concentration inside the vesicle of the positively charged species, $[P^+_{inside}]$, is zero as we focus on the initial rate. At low pH values, the concentration of the negatively charged species is negligible (eq 2) and we can therefore write for the initial rate at low pH

$$[TRP] \cong [P^+] + [Z^{+/-}] = [P^+] + \frac{K_1[P^+]}{[H^+]}$$

$$[P^+] = \frac{[TRP]}{[1 + K_1/[H^+]]}$$

Substituting in the expression for the rate, we identify the apparent rate coefficient, k, which is measured experimentally, and its relationship to the permeability coefficient, P.

$$\frac{d[TRP]}{dt} = -\frac{PA}{V}\frac{[H^+]}{[H^+] + K_1}[TRP] = -k[TRP]$$

$$P = \frac{kV}{A}\left[1 + \frac{K_1}{[H^+]}\right] \tag{5}$$

We now extract from the experiment an estimate of the permeation coefficient. The rate coefficient at pH 2.4 is $k \cong 0.033/60\ s^{-1}$. We consider the low pH results for our fit due to significantly lower error bars compared to other pH measurements. The total volume of the prepared solution is 400 μL. This solution includes 1.81×10^{19} DOPC molecules. The total surface area of these lipid molecules, exposed to the external solvent, is $72.1 \times (1.81 \times 10^{19}) \times (10^{-16})/2 = 65250.5\ cm^2$, where 72.1 Å^2 is the surface area of a single head.[17] Assuming that all the DOPC molecules are incorporated in vesicles and substituting in the expression for the permeation coefficient (eq 5), we have for pH 2.4

$$P \cong \frac{0.033 \times 400 \times 10^{-3}}{60 \times 65250.5}\left[1 + \frac{4.17 \times 10^{-3}}{10^{-2.4}}\right]$$

$$= 6.9 \times 10^{-9}\ cm/s \tag{6}$$

III.2. Simulations. Figure 3 shows the potential of mean force for permeation of different ionic species of tryptophan molecules through the DOPC bilayer membrane. The origin ($Z = 0$) is the center of the membrane. For all of the species, the

DOI: 10.1021/acs.jpcb.5b02122
J. Phys. Chem. B XXXX, XXX, XXX−XXX

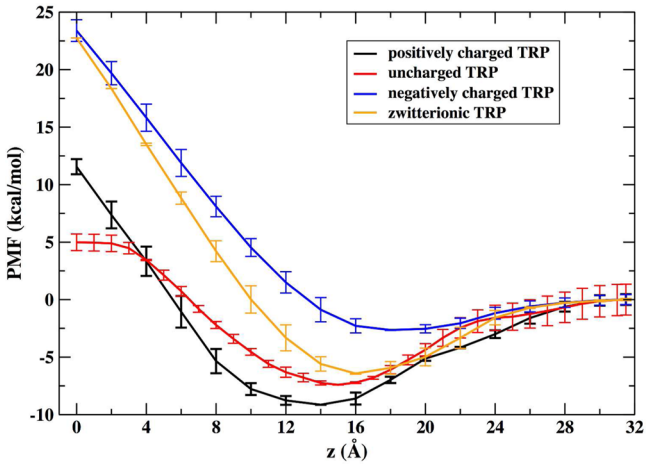

Figure 3. Free energy profile for the penetration of the different tryptophan species as a function of distance from the membrane center. Error bars are estimated by computing the energies for the two leaflets of the bilayer. The energies are shifted so they are zero farther away from the membrane.

barrier for permeation is located at the center of the membrane. This barrier is significantly larger for the permeation of the negatively charged tryptophan and the zwitterionic molecule compared to the positively charged species. This is in qualitative agreement with the reported experimental observation. For the positively charged species, the barrier at the center is about 10 kcal/mol lower and the barrier is even smaller for the permeation of a neutral tryptophan molecule. These free energy profiles also show that the positively charged tryptophan binds more strongly to the membrane (with a minimum at a location 14 Å away from the membrane center) than the other species. This binding interaction is very weak for the negatively charged tryptophan. Weaker binding of anions compared to cations has been observed before in constrained simulations. An example is binding to the surface of the membrane by sodium and chloride ions[37] or the permeation of these ions through the membrane.[38−40] Recent experiments and simulations suggest a similar membrane binding for both atomic ions.[41] The barrier for permeation measured from the binding locations in the membrane is 12.4 ± 0.7, 20.7 ± 0.7, 26.0 ± 0.9, and 29.2 ± 0.1 kcal/mol for the neutral, positively charged, negatively charged, and zwitterionic tryptophan species, respectively.

Since the equilibrium free energy profiles are not easy to measure, we estimate below the value of the permeation coefficients that is frequently determined experimentally.[42]

Table 1 shows the permeability coefficients for the three charged molecules of tryptophan computed with the solubility-diffusion model[26,27]

$$P = \left[\int_{z_1}^{z_2} \frac{\exp(\beta \Delta G(z))}{D(z)}\, dz\right]^{-1}$$

where $D(z)$ is a position dependent diffusion coefficient for the permeant along the membrane axis z, that we computed from our simulations using

$$D(z) = \frac{(RT)^2}{\int_0^\infty \langle \Delta F_z(z, t) \Delta F_z(z, 0)\rangle\, dt}$$

Table 1. Permeability Coefficients for Tryptophan Permeation with Different Charges[a]

permeant	permeability coefficient (cm/s)
zwitterionic tryptophan	6.27×10^{-16} to 4.90×10^{-15}
positively charged tryptophan	9.5×10^{-8} to 4.2×10^{-6}
negatively charged tryptophan	1.13×10^{-16} to 1.63×10^{-14}

[a]The range of values is estimated by computing the permeation independently for each half of the membrane. Note the significant range of values and that the permeation of the positively charged species is significantly larger in accord with experiment. The absolute value of the simulated permeation, however, is significantly larger than the experimental estimate.

with $\Delta F_z(z, t)$ being the instantaneous deviation of the constrained force $F_z(z,t)$ from the average force $\langle F_z(z)\rangle$.

Table 1 shows that the permeability coefficients for the zwitterionic and negatively charged tryptophan are very low with values similar to the permeabilities estimated previously for other ionic species.[43−45] In contrast, the permeability of the positively charged tryptophan is 9 orders of magnitude larger. Assuming that these charged species do not change their protonation state during insertion and diffusion through the membrane, those permeability estimates suggest that the only molecule that can move through the membrane is the positively charged tryptophan.

To assess the computed values, we compared values of the diffusion constant to other reported values. Landolt-Börnstein reported a value of 0.66×10^{-5} cm^2/s for tryptophan in water.[46] Mark and Nilsson[47] found the diffusion coefficient for tryptophan in water to be in the range 13×10^{-5} to 4×10^{-5} cm^2/s. Our computations estimate diffusion coefficients in water as 6×10^{-5} and 8×10^{-5} cm^2/s for the positively and negatively charged species, respectively. Hence, our simulations are similar to other calculations and are about an order of magnitude faster than experimental measurements. These deviations are quite typical in the field.

What is the mechanism that makes the permeation of the positively charged tryptophan so different compared to the permeation of the other two charged species? To answer this question, we consider the changes of membrane structure that occur when any of the three species are close to the membrane center (Figures 4−6). For all permeants, we observe a defect of water permeation that accompanies the permeant and is widely known in the field of permeant−membrane interactions.[8,43,44] Significant variation in the sizes and characteristics of the defects is found for the tryptophan species. When the zwitterionic and negatively charged molecules are closer to the membrane center, up to 15 water molecules accompany the permeant to compensate for the large energetic penalty of having those charged species in the hydrophobic core of the membrane (Figures 4 and 5). On average, only six water molecules follow the positive species, suggesting a smaller water perturbation.

Some modifications to the membrane structure are also observed. For example, for the negatively charged species, and with less extent for the zwitterionic moiety, one choline group attempts to approach the permeant located at the center of the membrane (Figure 5a,b). Since the choline is right at the top of the DOPC molecule, the potential interruption to the membrane structure is significant and is very rare (see also Figure 6c). The membrane perturbation is different when the positively charged tryptophan is closer to the membrane center.

DOI: 10.1021/acs.jpcb.5b02122
J. Phys. Chem. B XXXX, XXX, XXX−XXX

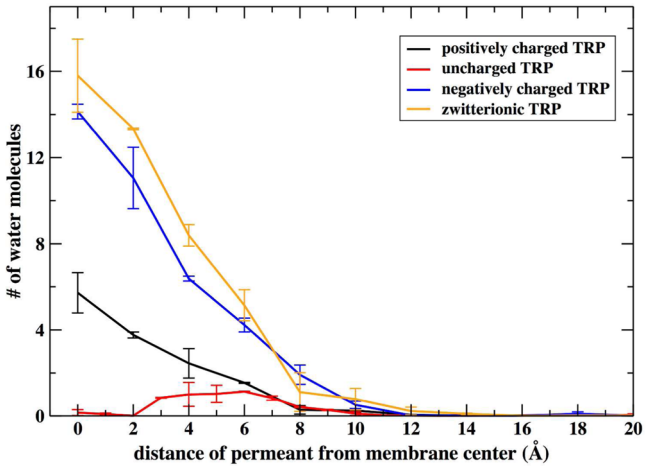

Figure 4. Number of water molecules that come closer than 10 Å from the membrane center plotted as a function of the location of the respective permeant. More than twice the number of water molecules penetrates to the membrane hydrophobic core when the zwitterionic or negatively charged tryptophan molecules are deeper inside the membrane compared to the water penetration for the positively charged tryptophan. In contrast, when an uncharged tryptophan is at the membrane center, water molecules remain away from that region. This observation suggests a significantly less disruptive permeation for the neutral and positively charged species compared to the negative ions and zwitterions.

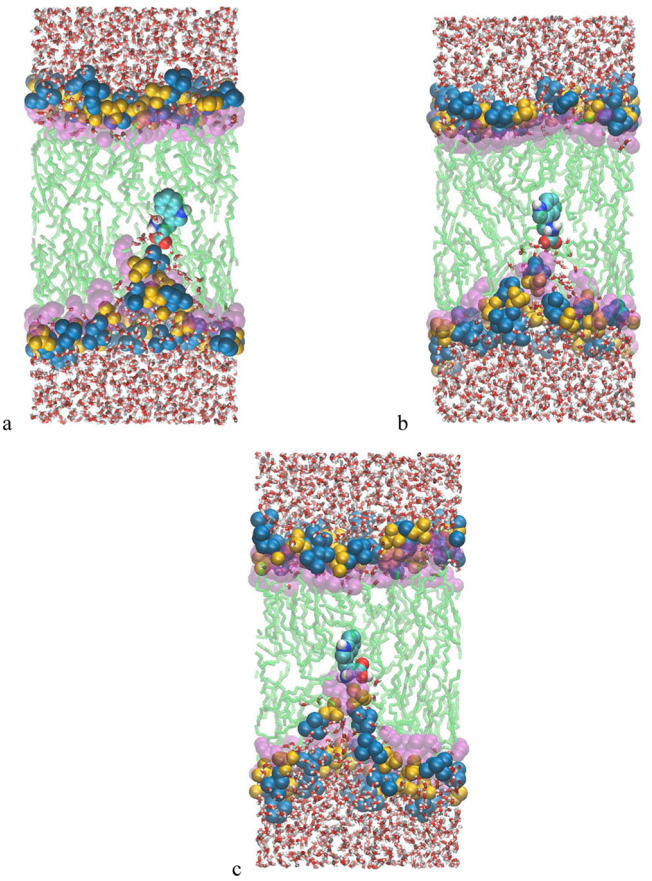

Figure 5. Representative molecular snapshots for a zwitterionic (a), negatively charged (b), and positively charged (c) tryptophan inserted in the middle of the membrane. A space filled representation is used for the tryptophan (with carbon atoms in cyan, oxygen in red, nitrogen in blue, and hydrogen in light gray), the phosphate (yellow), the choline (dark blue), and the glycerol (clear purple) groups of the lipid molecules. The hydrophobic lipid tails are colored in green, and the water atoms at the top and bottom are in red and light gray. See text for more details. These molecular snapshots were prepared with the program VMD.[48]

In this case, usually two phosphate groups (that are more centered compared to the choline group) remain closer to the permeant as well as accompany glycerol groups that surround the positively charged amino group (Figures 5c and 6a,b) and help stabilize the ion. Hence, rather than deformation of mostly membrane components which is induced by a positive permeant (sliding of phosphate and glycerol groups toward the center), a negative or zwitterion permeant requires membrane disruption and the entry of a significant number of water molecules for charge compensation. The last is illustrated to be more costly by the PMF calculations (Figure 3).

The membrane distortions observed in the simulations modify the electrostatic interactions felt by the charged permeants. Figure 7 shows the electrostatic energy of the charged permeant while it moves across the membrane axis. For the positively charged tryptophan, the electrostatic interaction is favorable when the permeant moves inside the membrane due to attractive interactions with several phosphate and glycerol groups (Figures 5 and 6). Closer to the membrane center, contacts with those charged and polar groups become more difficult and the energy increases. Contrasting with these results, a negatively charged tryptophan feels an increasing unfavorable energy moving to the membrane center after it crosses the area where the positive charged choline groups are located (about 20−24 Å from the membrane center). This suggests that the membrane distortions that would be required to compensate for the electrostatic penalty for the permeation of this negative ion, specifically the approach of several choline groups, are more costly than the observed approach of phosphate and glycerol groups to interact with a positively charged tryptophan.

We expect that a neutral permeant will perturb the membrane less. We therefore also consider membrane perturbation by a neutral, uncharged tryptophan. To examine the impact of membrane structure on permeation of charged species, we replace the uncharged tryptophan in the MD sampled structures by the charged species and compute the electric field experienced by the permeant. The results are also reported in Figure 7. The electrostatic energy as a function of the membrane depth of the permeant has similar but weaker trends compared to the energy profiles sampled in simulations of charged species permeation. Interestingly, when unperturbed membrane is considered (i.e., membrane without a permeant) and an ion is simply placed at different membrane positions along the normal, the electrostatic energy flips. Negatively charged ions are preferred by the unperturbed membrane in accord with Clarke's argument. Previous simulation studies of pure lipid bilayers[49−51] have shown that this preference is due to the positive potential contribution of the oriented water molecules located at the membrane/water interface that overcompensate the negative potential contribution of the lipid head groups. Hence, it is the membrane distortion induced by the permeant that selects positively charged ions.

DOI: 10.1021/acs.jpcb.5b02122
J. Phys. Chem. B XXXX, XXX, XXX−XXX

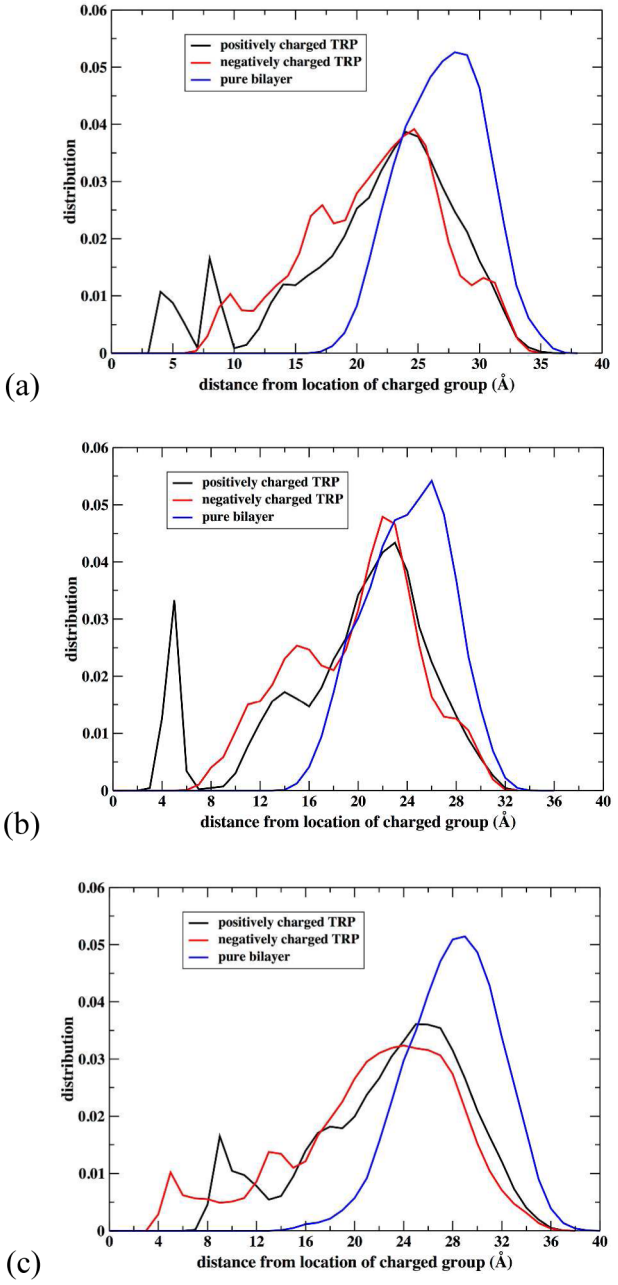

Figure 6. Radial distribution functions for (a) phosphate, (b) glycerol, and (c) choline groups with respect to the location of the charged group in the permeant. In these figures, the center of mass of the permeant is at the membrane center. Note the significant glycerol peak for the positively charged permeant suggesting a significant screening effect. No such membrane group is found to support the negatively charged or zwitterion species. The plots also show the regular distribution of these groups in an unperturbed membrane.

IV. CONCLUSIONS

In this paper, we illustrate, using a combination of experiments and simulations, the high efficiency of permeation of positively charged peptides compared to negatively charged ions or to zwitterions. This observation is surprising given the overall hydrophobic structure of the membrane moiety that has no significant electric interactions. Furthermore, this observation is also in disagreement with earlier investigations of transport of organic ions that suggest anions as the better permeating species. An explanation to this challenge is provided by detailed analysis of the MD simulations, results that are also consistent with the experiments we have conducted.

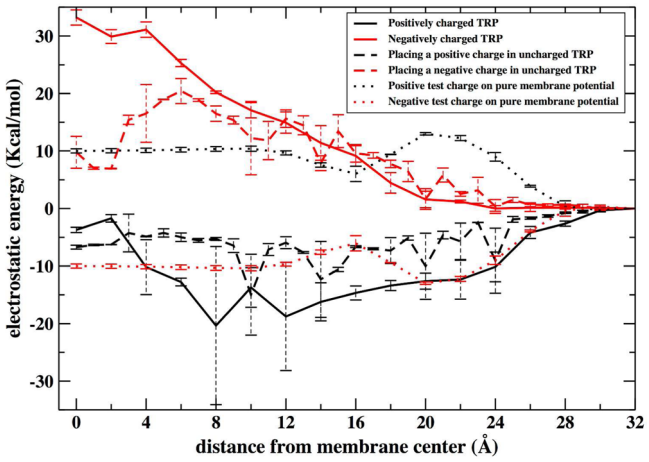

Figure 7. Electrostatic energy change on a translocating positive charge (black) or negative charge (red) moving inside the membrane. Alternate membrane sampling by molecular dynamics simulations is considered. The energy seen by the positive and negative charged tryptophan during sampling of system configurations of those charged peptides are shown with solid lines. Sampling membrane configurations by neutral tryptophan and then computing the energy of a positive charge placed on the nitrogen of the amino group or of a negative charge placed on the hydroxyl group of an uncharged tryptophan is shown with dashed lines. Finally, configuration samples of a pure DOPC membrane (no permeant) are used to place a point charge moving across an unperturbed membrane shown with dotted lines. Error bars are estimated by computing the electrostatic energies for the two leaflets of the bilayer. The energies were shifted so they are all zero farther away from the membrane center. Note that the electric field computed without the permeant has an opposite tendency to perturbed membrane. It prefers transporting negative ions and not positively charged species. The unperturbed membrane results are in accord with the transport of organic ions[31] and Clarke's theory.[13]

We have shown that permeation is enhanced by defect formation in the membrane. The positively charged permeants effectively pull the negatively charged phosphate and the polar glycerol groups in the direction of the membrane center. The last two groups ease the electrostatic self-energy felt by the permeant in the low dielectric environment. In contrast, negatively charged ions are less successful in pulling the (further away) positively charged choline groups. To compensate the high self-energy in the low dielectric environment, anions induce membrane disruption and gather a significant number of water molecules around them. The disruption is significantly more costly in energy than the internal membrane distortion found for cations. We note that if the membrane is unperturbed a reverse trend is obtained; negative ions are more permeable than positive ions. This explains why organic anions, which are likely to have a small effect on the hydrophobic core of the membrane, translocate better than organic cations.

It will be of considerable interest to conduct additional experiments with one of the peptide ends blocked, reducing the impact of very different pH's on the environment.

AUTHOR INFORMATION

Notes

The authors declare no competing financial interest.

DOI: 10.1021/acs.jpcb.5b02122
J. Phys. Chem. B XXXX, XXX, XXX−XXX

■ ACKNOWLEDGMENTS

The authors acknowledge the Texas Advanced Computing Center (TACC) at the University of Texas at Austin for providing HPC resources that have contributed to the results reported within this paper (URL:http://www.tacc.utexas.edu). This research was supported by a Welch Foundation grant F-1783 and NIH grant GM59796 to R.E. and Welch Foundation grant F-1722 to L.J.W.

■ REFERENCES

(1) Alberts, B.; Johnson, A.; Lewis, J.; Raff, M.; Roberts, K.; Walter, P. *Molecular Biology of the Cell*; Garland Science: New York, 2008.
(2) Tepper, H. L.; Voth, G. A. Mechanisms of Passive Ion Permeation through Lipid Bilayers: Insights from Simulations. *J. Phys. Chem. B* **2006**, *110*, 21327−21337.
(3) Aqvist, J.; Warshel, A. Simulation of Enzyme Reactions Using Valence Bond Force Fields and Other Hybrid Quantum/Classical Approaches. *Chem. Rev.* **1993**, *93*, 2523−2544.
(4) Khavrutskii, I. V.; Gorfe, A. A.; Lu, B. Z.; McCammon, J. A. Free Energy for the Permeation of Na+ and Cl- Ions and Their Ion-Pair through a Zwitterionic Dimyristoyl Phosphatidylcholine Lipid Bilayer by Umbrella Integration with Harmonic Fourier Beads. *J. Am. Chem. Soc.* **2009**, *131*, 1706−1716.
(5) Lazaridis, T.; Leveritt, J. M.; PeBenito, L. Implicit Membrane Treatment of Buried Charged Groups: Application to Peptide Translocation across Lipid Bilayers. *Biochim. Biophys. Acta, Biomembr.* **2014**, *1838*, 2149−2159.
(6) Herce, H. D.; Garcia, A. E. Molecular Dynamics Simulations Suggest a Mechanism for Translocation of the Hiv-1 Tat Peptide across Lipid Membranes. *Proc. Natl. Acad. Sci. U.S.A.* **2007**, *104*, 20805−20810.
(7) Herce, H. D.; Garcia, A. E. Cell Penetrating Peptides: How Do They Do It? *J. Biol. Phys.* **2007**, *33*, 345−356.
(8) MacCallum, J. L.; Bennett, W. F. D.; Tieleman, D. P. Distribution of Amino Acids in a Lipid Bilayer from Computer Simulations. *Biophys. J.* **2008**, *94*, 3393−3404.
(9) Dorairaj, S.; Allen, T. W. On the Thermodynamic Stability of a Charged Arginine Side Chain in a Transmembrane Helix. *Proc. Natl. Acad. Sci. U.S.A.* **2007**, *104*, 4943−4948.
(10) Yoo, J.; Cui, Q. Does Arginine Remain Protonated in the Lipid Membrane? Insights from Microscopic Pk(a) Calculations. *Biophys. J.* **2008**, *94*, L61−L63.
(11) Li, L. B.; Vorobyov, I.; Allen, T. W. The Different Interactions of Lysine and Arginine Side Chains with Lipid Membranes. *J. Phys. Chem. B* **2013**, *117*, 11906−11920.
(12) Gleason, N. J.; Vostrikov, V. V.; Greathouse, D. V.; Koeppe, R. E. Buried Lysine, but Not Arginine, Titrates and Alters Transmembrane Helix Tilt. *Proc. Natl. Acad. Sci. U.S.A.* **2013**, *110*, 1692−1695.
(13) Clarke, R. J. The Dipole Potential of Phospholipid Membranes and Methods for Its Detection. *Adv. Colloid Interface Sci.* **2001**, *89*, 263−281.
(14) Vorobyov, I.; Bekker, B.; Allen, T. W. Electrostatics of Deformable Lipid Membranes. *Biophys. J.* **2010**, *98*, 2904−2913.
(15) Chakrabarti, A. C. Permeability of Membranes to Amino-Acids and Modified Amino-Acids - Mechanisms Involved in Translocation. *Amino Acids* **1994**, *6*, 213−229.
(16) Chakrabarti, A. C.; Deamer, D. W. Permeability of Lipid Bilayers to Amino-Acids and Phosphate. *Biochim. Biophys. Acta* **1992**, *1111*, 171−177.
(17) Liu, Y. F.; Nagle, J. F. Diffuse Scattering Provides Material Parameters and Electron Density Profiles of Biomembranes. *Phys. Rev. E* **2004**, *69*, 040901-1−040901-4.
(18) Jorgensen, W. L.; Tiradorives, J. The Opls Potential Functions for Proteins - Energy Minimizations for Crystals of Cyclic-Peptides and Crambin. *J. Am. Chem. Soc.* **1988**, *110*, 1657−1666.
(19) Berger, O.; Edholm, O.; Jahnig, F. Molecular Dynamics Simulations of a Fluid Bilayer of Dipalmitoylphosphatidylcholine at Full Hydration, Constant Pressure, and Constant Temperature. *Biophys. J.* **1997**, *72*, 2002−2013.
(20) Berendsen, H. J. C.; Grigera, J. R.; Straatsma, T. P. The Missing Term in Effective Pair Potentials. *J. Phys. Chem.* **1987**, *91*, 6269−6271.
(21) Essmann, U.; Perera, L.; Berkowitz, M. L.; Darden, T.; Lee, H.; Pedersen, L. G.; Smooth, A. Particle Mesh Ewald Method. *J. Chem. Phys.* **1995**, *103*, 8577−8593.
(22) Weinbach, Y.; Elber, R. Revisiting and Parallelizing Shake. *J. Comput. Phys.* **2005**, *209*, 193−206.
(23) Ryckaert, J. P.; Ciccotti, G.; Berendsen, H. J. C. Numerical Integration of Cartesian Equations of M Otion of a System with Constraints - Molecular Dynamics of N-Alkanes. *J. Comput. Phys.* **1977**, *23*, 327−341.
(24) Tuckerman, M.; Berne, B. J.; Martyna, G. J. Reversible Multiple Time Scale Molecular-Dynamics. *J. Chem. Phys.* **1992**, *97*, 1990−2001.
(25) Cardenas, A. E.; Jas, G. S.; DeLeon, K. Y.; Hegefeld, W. A.; Kuczera, K.; Elber, R. Unassisted Transport of N-Acetyl-L-Tryptophanamide through Membrane: Experiment and Simulation of Kinetics. *J. Phys. Chem. B* **2012**, *116*, 2739−2750.
(26) Marrink, S. J.; Berendsen, H. J. C. Simulation of Water Transport through a Lipid-Membrane. *J. Phys. Chem.* **1994**, *98*, 4155−4168.
(27) Marrink, S. J.; Berendsen, H. J. C. Permeation Process of Small Molecules across Lipid Membranes Studied by Molecular Dynamics Simulations. *J. Phys. Chem.* **1996**, *100*, 16729−16738.
(28) Kirmizialtin, S.; Elber, R. Computational Exploration of Mobile Ion Distributions around Rna Duplex. *J. Phys. Chem. B* **2010**, *114*, 8207−8220.
(29) Straub, J. E.; Thirumalai, D. Exploring the Energy Landscape in Proteins. *Proc. Natl. Acad. Sci. U.S.A.* **1993**, *90*, 809−813.
(30) Wang, L. G. Measurements and Implications of the Membrane Dipole Potential. *Annu. Rev. Biochem.* **2012**, *81*, 615−635.
(31) Liberman, Y. A.; Topaly, V. P. Permeability of Bimolecular Phospholipid Membranes for Fat-Soluble Ions. *Biofizika* **1969**, *14*, 452−461.
(32) Hu, Y.; Ou, S. C.; Patel, S. Free Energetics of Arginine Permeation into Model Dmpc Lipid Bilayers: Coupling of Effective Counterion Concentration and Lateral Bilayer Dimensions. *J. Phys. Chem. B* **2013**, *117*, 11641−11653.
(33) Ou, S. C.; Lucas, T. R.; Zhong, Y.; Bauer, B. A.; Hu, Y.; Patel, S. Free Energetics and the Role of Water in the Permeation of Methyl Guanidinium across the Bilayer-Water Interface: Insights from Molecular Dynamics Simulations Using Charge Equilibration Potentials. *J. Phys. Chem. B* **2013**, *117*, 3578−3592.
(34) MacCallum, J. L.; Bennett, W. F. D.; Tieleman, D. P. Transfer of Arginine into Lipid Bilayers Is Nonadditive. *Biophys. J.* **2011**, *101*, 110−117.
(35) Huang, K.; Garcia, A. E. Free Energy of Translocating an Arginine-Rich Cell-Penetrating Peptide across a Lipid Bilayer Suggests Pore Formation. *Biophys. J.* **2013**, *104*, 412−420.
(36) Cullis, P. R.; Hope, M. J.; Bally, M. B.; Madden, T. D.; Mayer, L. D.; Fenske, D. B. Influence of Ph Gradients on the Transbilayer Transport of Drugs, Lipids, Peptides and Metal Ions into Large Unilamellar Vesicles. *Biochim. Biophys. Acta, Rev. Biomembr.* **1997**, *1331*, 187−211.
(37) Siva, K.; Elber, R. Ion Permeation through the Gramicidin Channel: Atomically Detailed Modeling by the Stochastic Difference Equation. *Proteins: Struct., Funct., Genet.* **2003**, *50*, 63−80.
(38) Bockmann, R. A.; Hac, A.; Heimburg, T.; Grubmuller, H. Effect of Sodium Chloride on a Lipid Bilayer. *Biophys. J.* **2003**, *85*, 1647−1655.
(39) Gurtovenko, A. A.; Vattulainen, I. Effect of Nacl and Kcl on Phosphatidylcholine and Phosphatidylethanolamine Lipid Membranes: Insight from Atomic-Scale Simulations for Understanding Salt-Induced Effects in the Plasma Membrane. *J. Phys. Chem. B* **2008**, *112*, 1953−1962.
(40) Valley, C. C.; Perlmutter, J. D.; Braun, A. R.; Sachs, J. N. Nacl Interactions with Phosphatidylcholine Bilayers Do Not Alter

DOI: 10.1021/acs.jpcb.5b02122
J. Phys. Chem. B XXXX, XXX, XXX−XXX

Membrane Structure but Induce Long-Range Ordering of Ions and Water. *J. Membr. Biol.* **2011**, *244*, 35−42.
(41) Knecht, V.; Klasczyk, B. Specific Binding of Chloride Ions to Lipid Vesicles and Implications at Molecular Scale. *Biophys. J.* **2013**, *104*, 818−824.
(42) Missner, A.; Pohl, P. 110 Years of the Meyer-Overton Rule: Predicting Membrane Permeability of Gases and Other Small Compounds. *ChemPhysChem* **2009**, *10*, 1405−1414.
(43) Wilson, M. A.; Pohorille, A. Mechanism of Unassisted Ion Transport across Membrane Bilayers. *J. Am. Chem. Soc.* **1996**, *118*, 6580−6587.
(44) Vorobyov, I.; Olson, T. E.; Kim, J. H.; Koeppe, R. E.; Andersen, O. S.; Allen, T. W. Ion-Induced Defect Permeation of Lipid Membranes. *Biophys. J.* **2014**, *106*, 586−597.
(45) Ulander, J.; Haymet, A. D. J. Permeation across Hydrated Dppc Lipid Bilayers: Simulation of the Titrable Amphiphilic Drug Valproic Acid. *Biophys. J.* **2003**, *85*, 3475−3484.
(46) Landolt-Bornstein, *Zahlenwerte Und Funktionen Aus Physik, Chemie, Astronomie, Geophysik Und Technik*; Springer: Berlin, 1969; Vol. *II*.
(47) Mark, P.; Nilsson, L. A Molecular Dynamics Study of Tryptophan in Water. *J. Phys. Chem. B* **2002**, *106*, 9440−9445.
(48) Humphrey, W.; Dalke, A.; Schulten, K. Vmd: Visual Molecular Dynamics. *J. Mol. Graphics Modell.* **1996**, *14*, 33−38.
(49) Saiz, L.; Klein, M. L. Electrostatic Interactions in a Neutral Model Phospholipid Bilayer by Molecular Dynamics Simulations. *J. Chem. Phys.* **2002**, *116*, 3052−3057.
(50) Vorobyov, I.; Allen, T. W. The Electrostatics of Solvent and Membrane Interfaces and the Role of Electronic Polarizability. *J. Chem. Phys.* **2010**, *132*, 185101-1−185101-13.
(51) Demchenko, A. P.; Yesylevskyy, S. O. Nanoscopic Description of Biomembrane Electrostatics: Results of Molecular Dynamics Simulations and Fluorescence Probing. *Chem. Phys. Lipids* **2009**, *160*, 63−84.
(52) Ruymgaart, A. P.; Cardenas, A. E.; Elber, R. MOIL-opt: Energy-Conserving Molecular Dynamics on a GPU/CPU System. *J. Chem. Theory Comput.* **2011**, *7*, 3072−3082.

DOI: 10.1021/acs.jpcb.5b02122
J. Phys. Chem. B XXXX, XXX, XXX−XXX